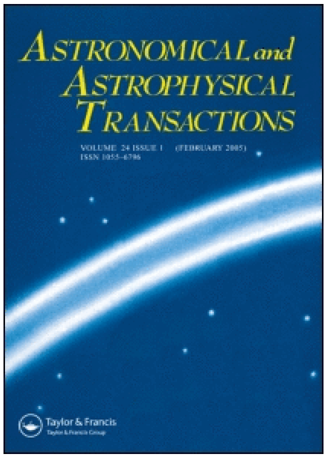

Astronomical & Astrophysical Transactions

The Journal of the Eurasian Astronomical Society

Publication details, including instructions for authors and subscription information:
http://www.informaworld.com/smpp/title~content=t713453505

Measuring the anisotropy in the CMB

L. A. Page [a]
[a] Physics Department, Princeton University, Princeton, NJ

Online Publication Date: 01 January 2000
To cite this Article: Page, L. A. (2000) 'Measuring the anisotropy in the CMB', Astronomical & Astrophysical Transactions, 19:3, 253 - 263
To link to this article: DOI: 10.1080/10556790008238575
URL: http://dx.doi.org/10.1080/10556790008238575

Astronomical and Astrophysical Transactions, 2000, Vol. 19, pp. 253–263
Reprints available directly from the publisher
Photocopying permitted by license only

MEASURING THE ANISOTROPY IN THE CMB

L. A. PAGE
Princeton University, Physics Department,
Jadwin Hall, Princeton NJ08544
E-mail: page@puppg.princeton.edu

(Received January 28, 2000)

The CMB is perhaps the cleanest cosmological observable. Its angular spectrum may be both computed and measured to percent accuracy. The current data clearly show a rise in the angular spectrum to a peak of roughly $\delta T_l = (l(l+1)C_l/2\pi)^{1/2} \approx 80$ μK at $l \approx 200$, and a fall at higher l. In particular, δT_l at $l = 400$ is significantly less than at $l = 200$. This is shown through a combined analysis of data sets and by the TOCO data alone.

For spatially flat models, a peak in the angular spectrum near $l = 200$ is indicated, whereas for $\Omega_0 = 0.35$ models one expects a peak near $l = 400$. The data clearly prefer the spatially flat models.

KEY WORDS CMB anisotropy, observations, spatially flat model

1 INTRODUCTION

These notes are from two talks given in St. Petersburg in August 1999. The goal was to assess the status of CMB anisotropy measurements, discuss some of the experimental techniques, and give some indication of what the future holds.

Figure 1 is a compendium of current anisotropy data. Some of the data have not been confirmed or are essentially unconfirmable; others have large calibration errors; still others have foreground contamination. Despite this, the trend is clear. From the Sachs–Wolfe plateau discovered by COME/DMR (Smoot *et al.*, 1992) there is a rise to an amplitude of $\delta T_l \approx 80$ μK at $l \approx 200$ and a fall after that.

There are multiple systematic checks between different experiments. At both large and small angular scales, the spectrum of the anisotropy is seen to be thermal. Also, at the largest angular scales, there is a clear correlation between DMR at 53 GHz and the FIRS data at 180 GHz (Ganga *et al.*, 1993). At smaller angular scales, SK at 35 GHz (Netterfield *et al.*, 1997) saw the same signal as did the MSAM experiment at 200 GHz. In an analysis tour de force, Fixsen *et al.* (1997)

*Presented on behalf of the Planck–LFI collaboration.

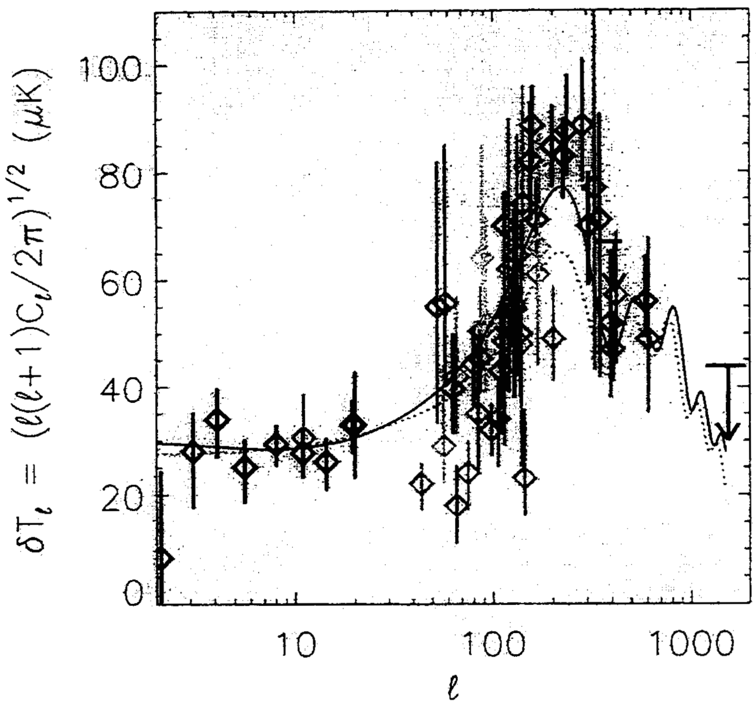

Figure 1 Unbiased sampling of data. The solid line on top is a model from Wang *et al.* (1999) with $\Omega_b = 0.05$, $\Omega_{cdm} = 0.3$, $\Omega_\Lambda = 0.65$, and $h = 0.65$. The dotted curve is the 'standard cold dark matter' model, which is inconsistent with many non-CMB observations, with $\Omega_b = 0.05$, $\Omega_{cdm} = 0.95$, $\Omega_\Lambda = 0.0$, and $h = 0.5$. Individual experiments are discussed by Halpern and Scott (1999).

showed that the COBE/FIRAS absolute spectrophotometer measured the same anisotropy as the COBE/DMR differential microwave radiometer. A plot of the cross-correlation is consistent with a thermal spectrum from 90 to 300 GHz.

2 OBSERVATIONAL SETTING AND FOREGROUND EMISSION

Characterizing the anisotropy is challenging because one endeavours to measure microkelvin variations from an experiment near a 300 K Earth. Fortunately, the CMB is the brightest thing in the sky between 0.6 and 600 GHz; and fluctuations from emission from our Galaxy (for galactic latitudes $|b| > 20°$) are smaller than the fluctuations intrinsic to the CMB (Tegmark *et al.*, 1999), as shown in Figure 2.

We may get a sense of the scale of the corrections for foreground emission from the SK experiment which observed near the North Celestial Pole ($b = 25°$). The contribution to the original data set from foreground emission is 4% at 40 GHz

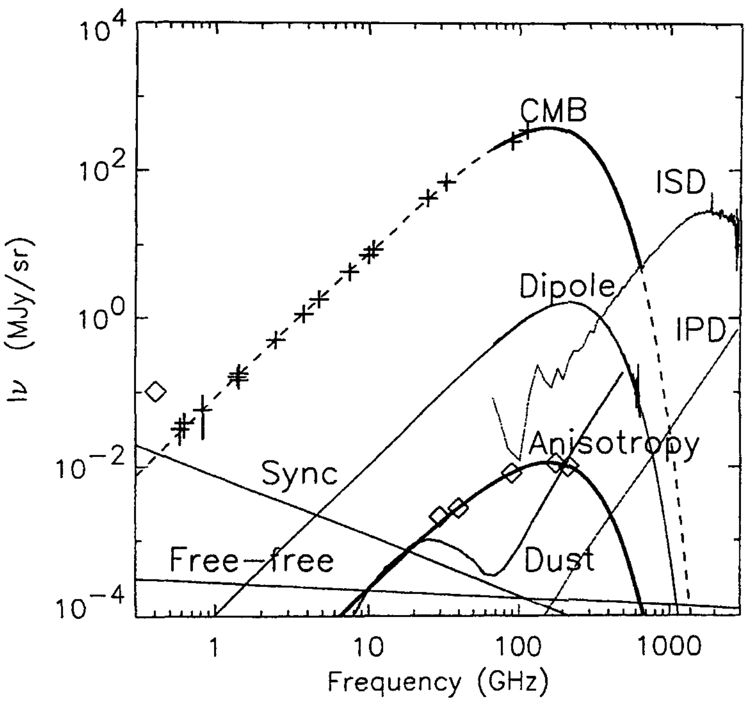

Figure 2 Plot of the CMB and the foreground emission at approximately the galactic latitude of the North Celestial Pole. For dust and synchrotron spectra, the fluctuating component has been plotted (de Oliveira-Costa *et al.*, 1998a). The flux levels of the free-free and dust emission have also been plotted. The corresponding l is about 20. At higher l, all these foregrounds have less fluctuation power. The FIRAS data (dust, dipole, and CMB spectra) are courtesy of Bill Reach.

(de Oliveira-Costa *et al.*, 1998a). It turns out the contamination was not due to free–free emission, Haslam-like synchrotron emission, or extra galactic sources, but rather it was due to a component correlated with interstellar dust emission. The favourite current explanation is that this component is radiation by spinning dust grains (Drain and Lazarian, 1999), but more measurements are required to be sure. Coble *et al.* (1999), looking in the southern hemisphere at high Galactic latitudes, found effectively no contamination at 40 GHz. At higher frequencies, the foreground emission has not been as thoroughly investigated.

3 TYPES OF MEASUREMENTS

The huge scientific payoff from characterizing the CMB has motivated over 20 experiments. There are three general measurement classes: (1) beam switching or beam synthesis experiments, (2) direct mapping experiments, and (3) interferometers. By far the most data have come from the beam switching/synthesis method, which is reviewed below, but this is certain to change soon with the new interferometers and balloon experiments coming on line.

The detectors of choice are high electron mobility transistor amplifiers (HEMTs Pospieszalski, 1992, 1997; Pospieszalski *et al.*, 1994) for frequencies below 100 GHz and bolometers for higher frequencies. The primary advantage of HEMTs is their ease of use and speed. A typical HEMT sensitivity is 0.5 mK $s^{1/2}$. The advantage of bolometers is their tremendous sensitivity, e.g. < 0.1 mK $s^{1/2}$. These devices are made by multiple groups though the JPL spider web bolometers are producing the best results. The CMB anisotropy has also been detected with SIS mixers (Kerr *et al.*, 1993).

4 MAT/TOCO: STATE-OF-THE-ART BEAM SWITCHING

As an example of a beam switching experiment, I'll discuss the TOCO data sets from the Mobile Anisotropy Telescope (MAT). This experiment is a collaboration between Mark Devlin's group at Penn and the Princeton group. We took the QMAP gondola (Delvin *et al.*, 1998) and optics, modified the cooling from liquid helium to a mechanical refrigerator, and mounted the telescope on a Nike Ajax radar trailer. For two seasons (October–December 1997 and June–December 1998) we observed from Cerro Toco near the ALMA site in the northern Chilean Andes.*

In this type of experiment, the beam is rapidly scanned across the sky over many beamwidths. In software, after the data are taken, the beam is synthesized. The experiment covers from $l = 60$ to $l = 400$ using six HEMT and two SIS detectors. The frequency range is from 30 to 150 GHz. In the field we were plagued by refrigerator problems. This resulted in a higher SIS temperature and thus lower sensitivity than we expected from the laboratory measurements.

In this sort of experiment, one must deal with the variable atmospheric temperature and variable local temperature. The data must be edited and one must go to great measures to ensure that the editing does not bias the answer. Of central importance is the correct assessment of the instrument noise. As δT_l^2 is proportional to the measured variance minus the instrument variance, an incorrect assessment of the noise will bias the result (see, for example Netterfield *et al.*, 1997 and Torbet *et al.*, 1999 for discussions).

The straightforward way to make sure that the noise is understood is to make combinations of the data in which the sky signal is cancelled out. The analysis of such a null signal should yield the instrument noise. These null combinations should cover multiple time scales and spatial scales. As an example, we show the null tests from the TOCO97 data in Figure 3 (for TOCO98 see Miller *et al.*, 1999). Note that in all cases, the signal is well above the instrument noise and that for each l-space bin, the null tests, regardless of time scale, give consistent noise levels.

*The Cerro Toco site of the Universidad Católica de Chile was made available through the generosity of Professor Hernán Quintana, Department of Astronomy and Astrophysics.

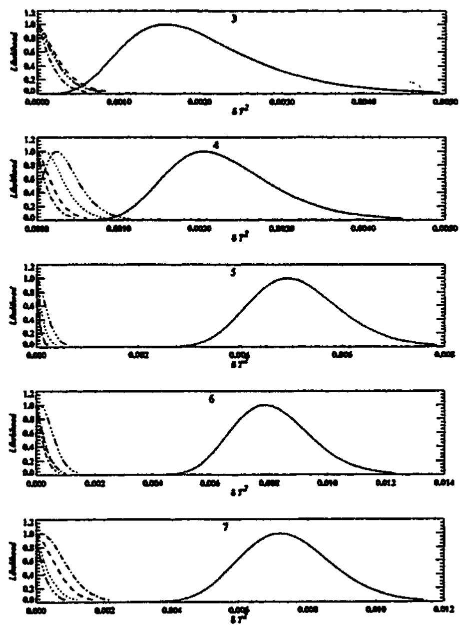

Figure 3 The likelihood of the data and the likelihood of the null combinations of the TOCO97 data set. The four null signals are data taken with the chopper scanning one way minus data with the chopper scanning the other, differences between subsequent 0.25 s segments, differences between subsequent 5 s segments, and the first half minus the second half of the campaign. From top to bottom, the panels correspond to $l = 63$, 86, 114, 158, and 199.

5 THE FUTURE

At $l < 1000$ the future is in multielement interferometers (Cosmic Background website; DASI website), long duration balloon flights e.g. (BOOMERanG websites), and satellite missions. At $l < 20$, the sky can only be mapped precisely from a satellite. For $l > 1000$, measurements can be made from the ground. Arrays of bolometers and interferometers seem ideal. The polarization has yet to be detected but experiments coming on line now should be able to do the job within a year or so.

There are now four space missions on the books. There is NASA's MAP satellite which just had its Launch-1 year review, there is ESA's Planck satellite (with collaborative NASA support) which is scheduled for a 2007 launch, there is the SPORT mission which plans to measure the polarization of the CMB at HEMT frequencies from the space station (Cortiglioni *et al.*, 1999), and, in NASA's technological road map, there is a mission, CMBPOL, to measure the polarization of the CMB in ≈ 2015. In the following, I shall focus on MAP because I know it best.

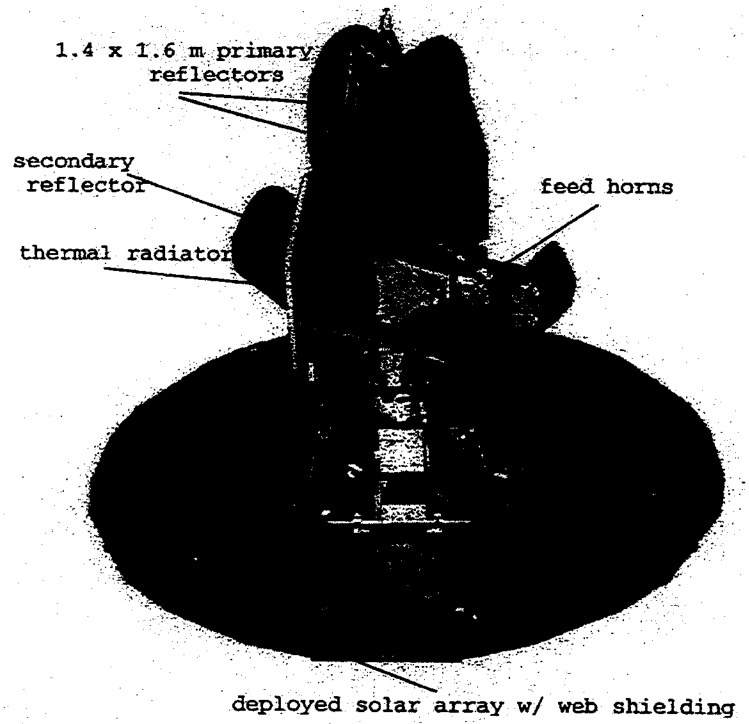

Figure 4 Picture of MAP with the solar arrays deployed. The receivers are located directly beneath the primary mirrors and are cooled by the thermal radiators. The Earth, Moon, and Sun are beneath the solar arrays.

6 MAP

The primary goal of MAP† is to produce a high fidelity, polarization sensitive, full sky map of the cosmic microwave background anisotropy. From its inception, the focus has been on how one makes a full sky map with negligible systematic error. MAP (Figure 4) is a MIDEX mission which means there is minimal redundancy as well as firm cost and schedule caps. MAP was proposed in June 1995, selected in April 1996, and is planned for a November 2000 launch. It was also proposed with the notion of getting the data to the community as fast as possible. We plan to make maps public nine months after we scan the whole sky (roughly one year after getting to L2).

Sources of systematic error in mapmaking include '$1/f$ noise' (any variations from tenths of seconds to minutes) in the detectors and instrument, magnetic fields,

†MAP is a collaboration between NASA (Chuck Bennett [PI], Gary Hinshaw, Al Kogut, and Ed Wollack), Princeton (Norm Jarosik, Michele Limon, Lyman Page, David Spergel and David Wilkinson), Chicago (Steve Meyer), UCLA (Ned Wright), UBC (Mark Halpern), and Brown (Greg Tucker).

and sidelobe contamination. Our systematic error budget allows for a total of 5 μK of extraneous signal *before* any modelling of the source of the contamination. The 5 μK applies to all angular scales and time scales though the most troublesome sources are the ones that are synchronous with the spin period.

6.1 Mission Outline

The design guidelines for MAP were:

- *Simplicity.* Other than the thruster valves and attitude control reaction wheels, there are no moving parts when the satellite is at L2. For taking science data, which should last a minimum of two years, there is only one mode of operation. MAP is passively cooled to $\approx$ 95 K. MAP'S mass is 800 kg and it uses 400 W.
- *Stability.* The orbit at the Earth–Sun Lagrange point, L2, is thermally stable and has a negligible magnetic field. L2 is roughly 1.5×10^6 km from Earth and the Sun, Earth, and Moon are always 'under' the spacecraft. (It will take approximately 3 months to get to L2.)
- *Heritage.* No major new components were required except the NRAO W-band amplifiers. These were designed for MAP.
- *Ease of Integration.* The mission relies on the complete understanding of the systematic noise levels. The magnitude of many of the systematic effects are easily determined when the instrument is warm.

6.2 Receivers

MAP continuously measures the difference in power from two input feeds on opposite sides of the spacecraft using pseudo-correlation radiometers. The essential elements are HEMT amplifiers designed by Marian Pospieszalski at the National Radio Astronomy Observatory (NRAO). The wide bandwidth and high sensitivity of the HEMTs, even while operating near 95 K, are what make MAP possible. There are ten feeds on each side of the spacecraft and each feed supports two polarizations, thus there are a total of 20 differential chains. Each receiver chain uses four amplifiers (two at $\approx$ 95 K and two at $\approx$ 290 K) for a total of 80 amplifiers. The radiometers are configured so that they difference two polarizations whose electric fields are parallel.

The key characteristic of the receivers is their low $1/f$ noise. The noise level at the spin rate, 8 mHz, is virtually the same as at the 2.5 kHz switching rate (the $1/f$ knee of the W-band HEMTs alone is near 1 kHz). This means that the receivers do not correlate noise from one pixel to the next (Table 1).

With a model of the receivers, and measurements that correlate the model to reality, we determine the sensitivity of the output to temperature variations in each component. The temperatures of the most sensitive components are monitored during flight to roughly 1 mK accuracy.

Table 1. MAP band centres and noise bandwidth.

Band	f_c *(GHz)*	*Bandwidth (GHz)*	*# Channels*
K	23	5.3	4
K_a	33	7	4
Q	41	8.4	8
V	61	12	8
W	95	17	16

Table 2. Approximate E and H plane beam θ_{FWHM}.

Band	θ_E *(deg)*	θ_H *(deg)*
K	0.95	0.75
K_a	0.7	0.6
Q	0.45	0.5
V	0.3	0.35
W	0.21	0.21

6.3 Optics

The optics comprises two back-to-back telescopes. The secondary of each telescope is illuminated by a cooled corrugated feed which is the input to the receiver chain. The reflector surfaces are shaped to optimize the beam profiles but to a good approximation, the telescopes are Gregorian.

The feeds and receivers occupy a large space. As a consequence the beam profiles are not symmetric (see Table 2). The scan strategy, to a first approximation, symmetrizes the beam profile. Thus even if the beams were 2-D Gaussians to start with, the symmetrized profile would not be Gaussian. Likewise, the window functions are not simply Gaussian. Nonetheless, the beam profiles and windows can be parametrized by Gaussians for most work. The data in the table are representative; the final beams will be measured in flight with sub-percent accuracy.

Outside of making the optics fit into the MIDEX fairing, one wants to ensure that one measures power from only the main beam. The Sun, Earth, and Moon, which are always at least 100° away from the main beam, are blocked by the solar arrays. The contribution from these sources is computed to be much less than 1 μK. The more difficult source to block is the Galaxy which illuminates the feeds from just over the top of the secondary. To block it, we substantially oversized the secondary, so that at its edge the illumination from the feed is less that 10^{-5} the illumination at the centre (< -50 dB edge taper).

The optics are modelled using a program, from YRS Associates [26] that solves for the currents on the reflectors as waves propagate through the system. The measured beam profiles (all have been measured at ten frequencies across the band)

Table 3. Approximate Galactic contributions for $|b| > 15°$.

Band	*Galactic contribution* (μK)	*Sidelobe contribution* (μK)
K	120	16
K_a	60	2
Q	40	4
V	20	0.2
W	...	...

are in excellent agreement with the predictions. Chris Barnes modified the code to run on a supercomputer so that we can also predict the sidelobes. The sidelobe measurements agree well with the predictions.

Using the models, we can estimate the contribution to MAP from the Galaxy. In the computer, we fly MAP over the Galaxy and record two signals. One signal is the rms difference between the two telescopes with the response integrated over the whole sky; the second signal is the same except with the contribution from the main beams subtracted. In other words, the second method tells how much Galactic signal comes through the sidelobes or from angles greater than $\approx 4°$ from the main beam. We do this for $|b| > 15$. The model is only approximate and does not yet include a contribution from extragalactic sources. Of course, the model will be updated after we measure what the Galaxy is really like.

To put these numbers in perspective, the rms magnitude of the CMB is about 120 μK. In K band, the rms Galaxy signal is roughly the same. To first order, these add in quadrature to produce a signal with an rms of 170 μK. In V-band, the galactic contribution is far less; it will change the power spectrum by $\approx 2\%$ if uncorrected. These rough numbers show that the power spectrum estimates are quite robust to the Galactic contamination. In producing a map of the CMB, we will clearly have to model and subtract the Galaxy. The rightmost column in Table 3 gives an indication of the contribution to the map if the sidelobe contribution is not accounted for.

6.4 Scan Strategy

To make maps that are equally sensitive to large and small scale structure, large angular separations must be measured with small beams. This is best done from L2. To guard against variations in the instrument, as many angular scales as possible should be covered in as short a time as possible. MAP spins and processes like a top. There are four time scales. The beams are differenced at 2.5 kHz; the satellite spins at 0.45 rpm; the spin axis processes around a 22.5° half-angle cone every hour; and the sky is fully covered in six months. In one hour, roughly 30% of the sky is mapped.

6.5 Science

Though the angular spectrum will be of great interest, it is not the best metric for assessing MAP. The primary goal is a map with negligible correlations between pixels and well understood (and small) systematic errors. With such a map, analyses are simplified and the map is indeed a true picture of the sky. MAP should be able to measure the temperature-polarization cross-correlation (Crittenden *et al.*, 1995) and will be sensitive to the polarization signal itself. Correlations with X-ray maps will shed light on the extended Sunyaev Zei'dovich effect (not to mention the dozen or so discrete sources (Refregier, 1998)). Correlations with the Sloan Digital Sky Survey will inform us about large-scale structure. MAP will be calibrated on the CMB dipole and thus will be able to calibrate radio sources and planets to a universal system. It will also help elucidate the emission properties of the intergalactic medium.

MAP will be sample variance limited up to $l \approx 700$. In other words, if the systematic errors and foreground contributions are under control, it will not be possible to determine the angular spectrum any better over this range. MAP will probe to $l \approx 1000$.

7 CONCLUSIONS

This is a truly amazing era for cosmology. Our theoretical knowledge has advanced to the point at which definite and testable predictions of cosmological models can be made. For the CMB anisotropy, results from the angular power spectrum, frequency spectrum, statistical distribution, and polarization must all be consistent. Using the CMB to probe cosmology is still in its early phase. Soon we will have precise cross-checks on the distribution, velocity flows, and masses of galaxies and clusters of galaxies as well as on the age of the universe. As cosmological models and measurements improve, the CMB and other measures will become a tool for probing high-energy physics.

References

BOOMERanG websites *http://oberon.roma1.infn.it/boomerang/* and *http://phobos.caltech.edu/~lgg/boom/boom.htm.*

Coble, K. *et al.* (1999) astro-ph/9902195.

Cortiglioni *et al.*. (1999) astro-ph/9901362.

Cosmic Background Imager *http://astro.caltech.edu/~tjp/CBI/.*

Crittenden, R. G., Coulson, D. and Turok, N. (1995) *Phys. Rev. D*, **52**, 5402. See also astro-ph/9408001 and astro-ph/9406046.

DASI website *http://astro.uchicago.edu/dasi/.*

de Oliveira-Costa, A., Devlin, M. J., Herbig, T. H., Miller, A. D., Netterfield, C. B., Page, L. A., and Tegmark, M. (1998a) *Astrophys. J. Lett.* **509**, 77.

de Oliveira-Costa, A., Tegmark, M., Page, L. A., and Boughn, S. (1998b) *Astrophys. J. Lett.* **509**, L9.

Devlin, M. J., de Oliveira-Costa, A., Herbig, T., Miller, A. D., Netterfield, C. B., Page, L. A., and Tegmark, M. (1998) *Astrophys. J. Lett.* **509**, L73.

Drain, B. T. and Lazarian, A. (1999) In: A. de Oliveira-Costa and M. Tegmark (eds.) *Microwave Foregrounds*, APS Conference Series, vol. 181, p. 133, ASP, San Francisco, astro-ph/9902356.

Fixsen, D. J. *et al.*. (1997) astro-ph/9704176.

Ganga, K. M. *et al.* (1993) *Astropys. J.* **432** L15.

Halpern, M. and Scott, D. (1999) In: A. de Oliveira-Costa and M. Tegmark (eds.) *Microwave Foregrounds*, APS Conference Series, vol. 181, p. 283, ASP, San Francisco.

Kerr, A. R., Pan, S-K., Lichtenberger, A. W., and Lloyd, F. L. (1993) *Proc. of the Fourth International Symposium on Space Terahertz Technology*, pp. 1–10.

MAXIMA website *http://cfpa.berkeley.edu/group/cmb/gen.html.*

Miller, A. D., Devlin, M. J., Dorwart, W., Herbig, T., Nolta, Page, L., Puchalla, J., Torbet, E., and Tran, H. (1999) *Astrophys. J. Lett.* **524**, L1.

Netterfield, C. B., Devlin, M. J., Jarosik, N., Page, L., and Wollack, E. J. (1997) *Astrophys. J.* 474, 47.

Pospieszalski, M. W. (1992) *Proc. IEEE Microwave Theory Tech.*, MTT-3 p. 1369.

Pospieszalski, M. W. (1997) In: F. R. Bouchet (ed.) *Microwave Background Anisotropies*, Editions Frontières, Gif-sur-Yvette, pp. 23–30.

Pospieszalski, M. W. *et al.* (1994) *IEEE MTT-S Digest*, 1345.

Refregier, A., Spergel, D., and Herbig, T. (1998) *Astrophys. J.*, astro-ph/9806349.

Smoot, G. F. *et al.* (1992) *Astrophys. J. Lett.* **396**, L1.

Tegmark, M. (1999) *Astropys. J.***514**, L69; see also astro-ph/9809201.

Tegmark, M., Eisenstein, D., Hu, W., and de Oliveira-Costa, A. (1999) *Astrophys. J.* (submitted) astro-ph/9905257.

Torbet, E., Devlin, M., Dorwart, W., Herbig, T., Nolta, J., Miller, A. D., Page, L., Puchalla, J., and Tran, H. (1999) *Astrophys. J. Lett.* **521**, L79, astro-ph/9905100.

Wang, L., Caldwell, R. R., Ostriker, J. P., and Steinhardt, P. J. (1999) astro-ph/9901388.

YRS Associates. Rahmat-Samii, Y., Imbriale, W., and Galindo, V. YRS Associates, 4509 Tobias Ave. Sherman Oaks, CA 91403.